Polymer Chemistry

Accepted Manuscript

ROYAL SOCIETY OF CHEMISTRY

www.rsc.org/polymers

Graphics for Contents

Fluorescent conjugated polymer based on thiocarbonyl quinacridone for sensing mercury ion and bioimaging

Yi Qu,[a,b] Xinran Zhang,[a] Yongquan Wu,[b] Fuyou Li[b] and Jianli Hua[a]**

Highly sensitive FRET-based thiocarbonyl quinacridone fluorescent conjugated polymers for sensing and bioimaging of mercury ion have been developed.

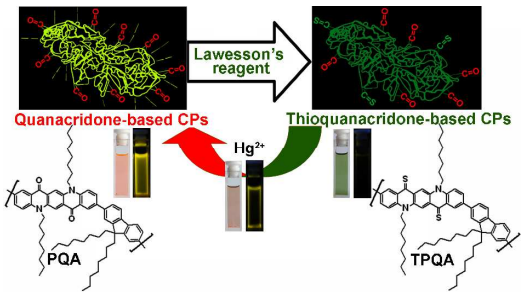

Fluorescent conjugated polymer based on thiocarbonyl quinacridone for sensing mercury ion and bioimaging

Yi Qu,[a,b] Xinran Zhang,[a] Yongquan Wu,[b] Fuyou Li[b] and Jianli Hua[a]**

[a]Key Laboratory for Advanced Materials and Institute of Fine Chemicals, East China University of Science and Technology, 130 Meilong Road, Shanghai 200237, P. R. China

[b]Department of Chemistry & Laboratory of Advanced Materials, Fudan University, 220 Handan Road, Shanghai, 200433, P. R. China

Emails: jlhua@ecust.edu.cn (Prof. Jianli Hua); fyli@fudan.edu.cn (Prof. Fuyou Li)

†Electronic supplementary information (ESI) available: The ^{1}H NMR, GPC data, IR spectra of four quinacridone-based polymers. The selectivity experimental figures of **PTQA2** and **PTQA-NPs**. See DOI:

Abstract

Because of the extreme toxicity of mercury ions (Hg^{2+}), a great deal of effort has been invested in developing probes that use colorimetric and fluorometric methods to detect them. Nowadays, most of the current fluorescent probes still work in the organic solvents or a mixture of organic solvents and water. Conjugated polymers (CPs) can serve as excellent fluorophores because of their strong emission and the controllable emission wavelength. In this work, a kind of thiocarbonyl quinacridone-based CPs nanoparticle (**PTQA-NPs**) was synthesized for selectively detecting Hg^{2+} in pure water. Additionally, the fabrication of nanoparticle provides a very sensitive correction for environmental effects, the minimum detectable concentration of Hg^{2+} for this nanoparticle was as low as 1 ppb. Furthermore, we show the capability of this polymer to monitoring Hg^{2+} in Hela cell lines by confocal laser scanning microscopy (CLSM).

Keywords: fluorescent probe; mercury ion; quinacridone; conjugated polymer nanoparticle; cell imaging

Introduction

The mercury ion (Hg^{2+}) is one of the most toxic metal ions because it can invade the nervous system, endocrine system and immune system of the organism.[1-4] Mercury can impair brain's cortex that caused central nerve system injury and dyskinesia. Embryo anamorphosis and mentally handicapped neonatorum also induced by infraction of mercury ion across the placenta.[5-7] Importantly, the concentration of the mercury pollutant is stored in animal tissues and not excreted that may be dramatically larger in the tissues of some animals at the top of a food chain.

A great deal of effort has been invested in developing easy-to-use colorimetric and fluorescent probes.[8-14] To achieve high selectivity, fluorescent chemodosimeters based on specific chemical reactions have been developed.[15-18] It is well-known that thioureas,[19,20] thioamides[21] and thiones[22] are all effective in reacting with mercury ion through the formation of the insoluble HgS deposits between the active C=S group and mercury ion. However, common commercial dyes in these researches showed poor stability under excitation in the presence of Hg^{2+} and oxygen. Quinacridone (QA) and its derivatives are widely used organic pigments with exceptional color and weather fastness.[23] Good light and temperature stability and high fluorescent quantum yield have permitted the fabrication of high performance organic fluorescent sensors based on QA derivatives. Two carbonyl groups on the skeleton of quinacridone can transfer to the thiolation analogue. Thiocarbonylquinacridone-based small molecular chemodosimeter for Hg^{2+} shows good selectivity and high detected limit (4.7 nM) that lower than the blood level (5.8 ppb) set by the U. S. EPA.[24] Furthermore, desulfurization of thiocarbonylquinacridone gives significant color change from dark green to bright red. As a

result, the derivative can be used as colorimetric probe for Hg^{2+}, which was seldom reported by previous studies.

It was well known that colorimetric and fluorescent probes based on water soluble CPs have attracted increasing attention and there are still challenges in this area.[25-29] Polyelectrolyte with amount of quaternary ammonium compounds is an useful strategy.[30] However, it is difficult to be modified on the insoluble pigment, such as quinacridone, which always need some more synthetic steps and lower yields. In another way, polymeric nanoparticles provide a widely universal fabrication method for hydrophobic and amphiphilic polymers.[31-36] In this work, we present the poly(fluorene-co-thiocarbonylquinacridone)-based colorimetric and fluorescent probe **PTQA-NPs** (Scheme 1) for sensing Hg^{2+} in both $CHCl_3$ solution (polymer solution) and PBS buffers (polymer nanoparticles).

This sensory system provides some advantages: (1) chemodosimeter was designed in this system which can reduce the interference from complex biocircumstance; (2) facile and simple synthesis. Suzuki couple reaction was chosen for synthesizing conjugated polymer and Lawesson's reagent was used for efficient surphuration of carbonyl group; (3) obviously fluorescent enhancement. This sensory system performed "turn on" response in blue (assigned to fluorene moiety) and orange (assigned to quinacridone moiety) channels. (4) high sensitivity. **PTQA-NPs** can detect Hg^{2+} in water at nM level.

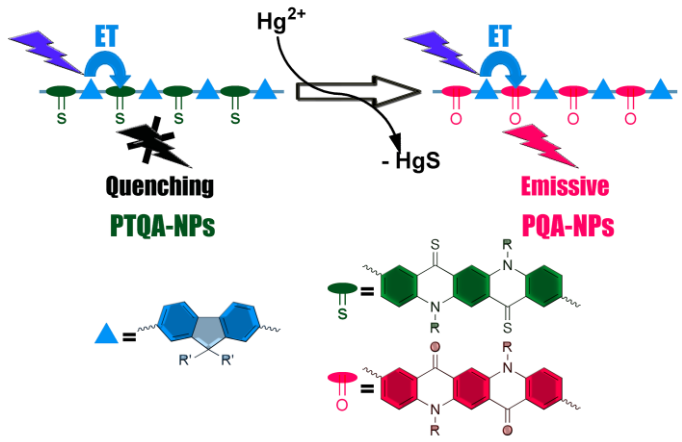

Scheme 1. Schematic illustration of the sensing process of ***PTQA-NPs*** to Hg^{2+} with changes in both colorimetric and fluorescent approaches.

Results and discussion

Design and principle of PTQA-NP for sensing Hg^{2+}

This work was designed on the basis of energy transfer (ET) process which (As shown in Scheme 1). The main chain of CPs alternated between fluorene and quinacridone moieties and ET process occurred in the main chain under excitation. Fluorene moiety acts as light harvesting group that can achieve ET process to quinacridone (emitter) or thiocarbonyl quinacridone (quencher). Moreover, fluorene can work as internal reference that exhibited blue emission around 480 nm when Hg^{2+} was added in the aqueous. Quinacridone showed strong emission in the orange-red to NIR channel (560 ~ 750 nm). Different amount of thiocarbonyl groups were induced as ET quencher by reacting polyquinacridone with different ratio of Lawesson's reagent. These thiocarbonyl groups on quinacridone skeleton were used for sensing Hg^{2+} and the ratio of C=S/C=O could modulate the origin fluorescent intensity of CPs. During the desulfurized process, the sulfur atom captured Hg^{2+} ion and generated the insoluble substance HgS(↓).

Meanwhile, the thiocarbonyl group was recovered to carbonyl group. As a result, the Hg^{2+} was cleared and fluorescence lighted up.

Synthesis

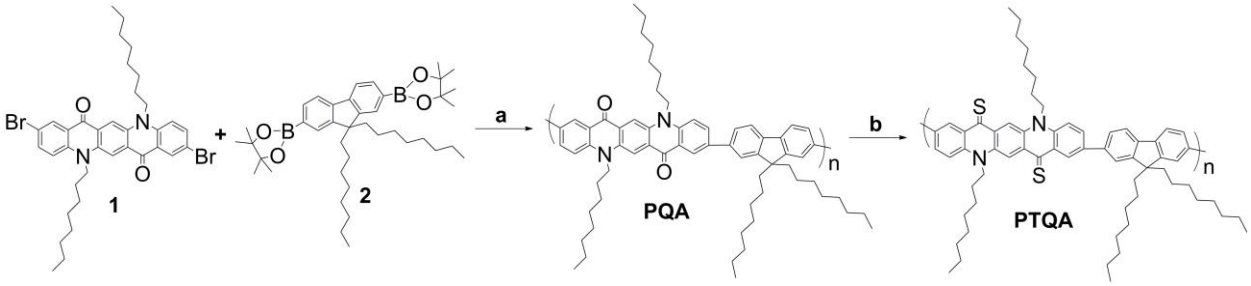

Figure 1. The synthetic routine of **PTQA** polymers. (a) $Pd(PPh_3)_4$, K_2CO_3, THF/H_2O; (b) Lawesson's reagent, toluene.

The synthetic route to **PQA** and **PTQA1~PTQA3** is illustrated in Figure 1. Monomer **1** is synthesized according to the previously published method.[24] Polymerization of **1** and 2,2'-(9,9-dioctyl-9H-fluorene-2,7-diyl)-bis(4,4,5,5-tetramethyl-1,3,2-dioxaborolane) (**2**) was carried out in the presence of palladium catalyst via the Suzuki cross-coupling reaction, providing the precursor polymer **PQA**. **PTQA1~PTQA3** with different thiolation rate could be obtained by a reaction of **PQA** with 0.4, 0.6 and 1.0 equiv. of Lawesson's reagent according to the literature with modification.[37]

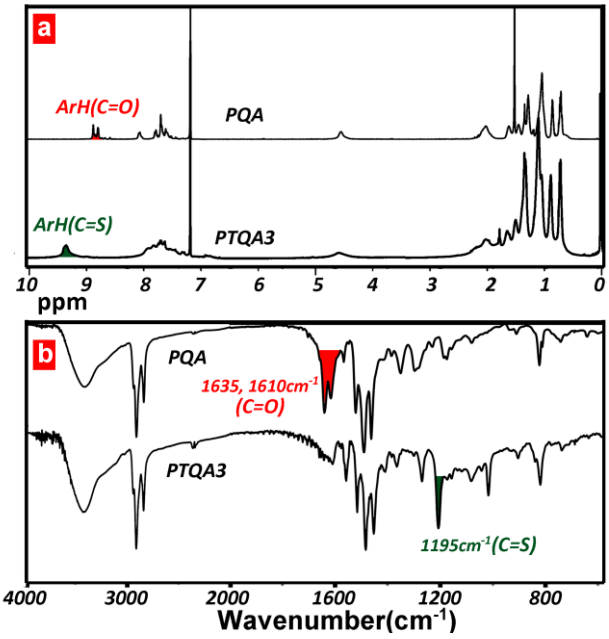

Figure 2. ^{1}H NMR and FT-IR spectra of **PQA** and **PTQA3**.

The ^{1}H NMR spectra of **PQA** and **PTQA1**~**PTQA3** were also used for determining the expected structure (see Figure 2a and Figure S1). As shown in Figure 2a, the ^{1}H NMR spectrum of **PQA** exhibited the peaks of phenylene group adjacent to C=O at 8.7–8.9 ppm and others of quinacridone group and fluorene group at 7.5–8.0 ppm. **PTQA1**~**PTQA3** with different amount of thiocarbonyl groups showed the signals decreased at 8.7–8.9 and increased peak around 9.4 (assigned to the protons adjacent to C=S moieties). We attempted to calculate the thiolated ratio from the integrations of both above peaks in the ^{1}H NMR spectra. Table S1 gives out a set of data of thiolated ratios for these three polymers: 26.3% (**PTQA1**), 66.7% (**PTQA2**), and 100% (**PTQA3**). The IR spectra of polymers were used for confirming the structure of **PQA** and its thiolate derivatives **PTQA1**~ **PTQA3**. As shown in Figure 2b, The IR spectrum of **PQA** showed the sharp peaks at 1635 cm^{-1} and 1610 cm^{-1} due to C=O stretching vibration from quinacridone skeleton. On the other hand, the stretching vibration peaks of C=S at 1195 cm^{-1} emerged in

PTQA3. These peaks can be found in **PTQA1** and **PTQA2,** indicating these polymers contained both C=O and C=S moieties (See Figure S2).

The GPC analysis revealed the weight average molecular weight (M_w) and polydispersity of **PQA** and **PTQA1**~**PTQA3** (Table S2). The molecular weights of these polymers are relatively low, which may be because the copolymerization reactivity of the quinacridone and fluorene monomers is not very high. A similar phenomenon can be seen in the previous report on polycondensation of the monomers.[38] Overall, the molecular weights are high enough for the polymer sensors to have good sensing properties.

Figure 3 showed the normalized UV-vis absorption (a) and photoluminescence spectra (b) of **PQA** and **PTQA1**~**PTQA3** in chloroform. **PQA** showed the characteristic absorption band at around 380, 505 and 545 nm in chloroform solution, which corresponded to the π-π* transitions of the fluorene segments and the quinacridone units, respectively. **PTQA3** showed the same absorption of fluorene at 383 nm but the absorption peak belonged to quinacridone was disappeared. The new absorption bands emerged at 623 and 680 nm were confirmed to absorption of dithiocarbonyl quinacridone chromophore in our previous report.[22] Similar absorption spectra were also found in the chloroform solutions of **PTQA1** and **PTQA2**, both of which showed the characteristic absorbance of quinacridone and thiocarbonyl quinacridone chromophores.

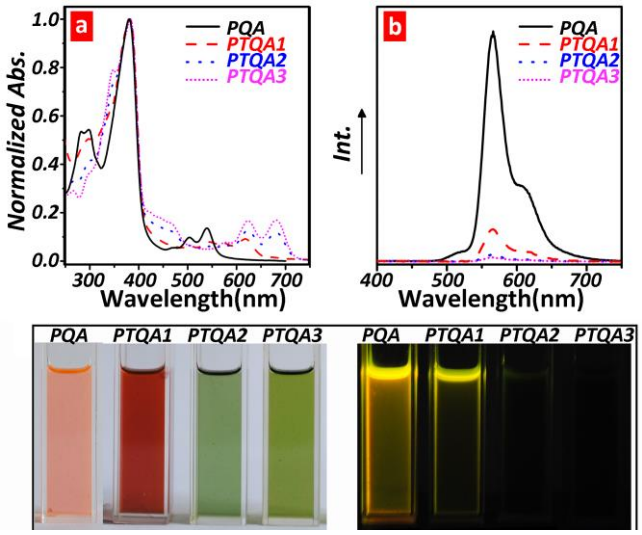

Figure 3. UV−vis absorption (a) and fluorescence spectra (b) of **PQA** and **PTQA1** ~ **PTQA3** in $CHCl_3$. Inset: color (a) and emission (b) pictures of **PQA** and **PTQA1**~**PTQA3**. [Polymer] = 10 μg/mL, λ_{ex} = 380 nm.

The emission intensities of **PQA**, **PTQA1**~**PTQA3** in chloroform were strongly dependent on the concentration of thiocarbonyl quinacridone units (Figure 3b). In a solution of **PQA**, a stronger orange emission at 566 nm can be observed, whose quantum yield was 0.905 by using rhodamine B as the reference. Furthermore, the quantum yields of **PTQA1**~**PTQA3** decreased to 0.122, 0.025 and 0.017, respectively. This phenomenon can be understood by intrachain exciton migration in chloroform solution and thiocarbonyl unit acted as exciton trap in the conjugated system.[39,40] It is worth pointing out that the obviously color changes and stronger emission quenching of quinacridone-containing polymers with different thiocarbonyl concentration in the solvent can be observed by the naked eye (photos in Figure 3). All of the photophysical data were listed in Table 1.

Table 1. Photophysical properties of **PQA**, **PTQA1~PTQA3**

No.	$\lambda_{abs.}$/nm	$\lambda_{em.}$/nm	Φ
PQA	380, 505, 545	566	0.905
PTQA1	382, 505, 545, 575, 623	566	0.122
PTQA2	382, 545, 575, 623, 680	563	0.025
PTQA3	383, 575, 623, 680	563	0.017

Nanoparticle morphology

With the efficient quenching of fluorescence and lower thiolated ratio, **PTQA2** was chosen to fabricate **PTQA-NPs**. The THF solution of **PTQA2** was dispersed in water by ultrasonication and indeed conveniently formed nanoparticles. The route for preparing **PTQA-NPs** is described in supporting information. The topographic properties of these homogeneousnano particles were studied by transmission electron microscopy (TEM) and atomic force microscopy (AFM) and Dynamic light scattering (DLS).

The morphology of **PTQA-NPs** nanoparticles in dry state was investigated by TEM and AFM after depositing onto cupper grid and mica, respectively. As shown in Figure 4a, ellipsoidal nanoparticles with an average diameter of 30 nm were observed by TEM. The AFM image in Figure 4b also shows the ellipsoidal morphology of **PTQA-NPs** nanoparticles with an average diameter of 50 nm. It was anticipated that the **PTQA-NPs** in aqueous solution with sub-50 nm diameter should be beneficial to perform detecting experiment in aqueous and cell uptake experiment. DLS measurement was further carried out to determine the hydrodynamic particle size of the whole nanoparticle range. The DLS measurements revealed that all the **PTQA-NPs** had a relatively narrow size distribution with a mean size of around 79±6 nm (Figure 5) in aqueous solution. The colloid particle diameter data obtained from TEM and AFM were

measured in the dry state while DLS result was the hydrodynamic diameter of the micelle measured in the solution state. Therefore, the particle sizes tested by TEM and AFM are smaller than that by DLS.

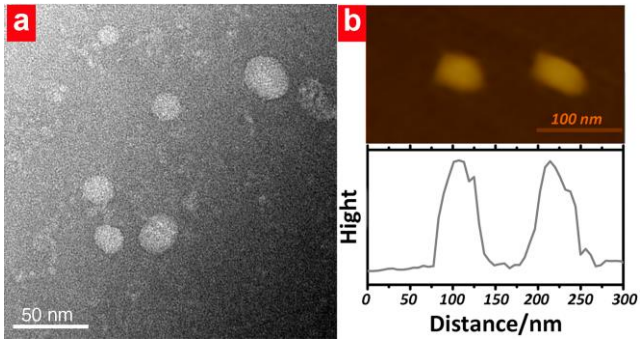

Figure 4. (a) TEM imagine of **PTQA-NPs**, carbon-coated copper grids, 1% phosphotungstic acid (PTA) negative stain; (b) AFM image with cross-sectional analysis of **PTQA-NPs**.

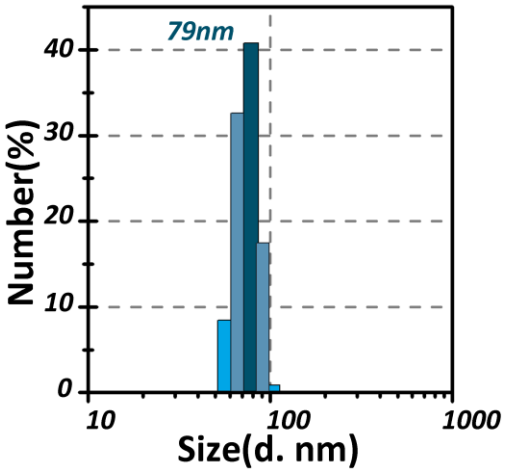

Figure 5. Histogram of the particle size distribution of **PTQA-NPs**.

Sensing Properties

The number of fluorescence-quenching groups plays an important role on the sensor capability. On the one hand, if there are not enough groups, the fluorescence cannot be fully quenched, resulting in an unsuccessful fluorescence-enhanced sensor; on the other hand, if there are too many groups, the sensor will lose its sensitivity because it can't release the fluorescence-

enhanced signal in time when the concentration of analyte is low. Although the thiolation rate of **PTQA3** is higher than that of **PTQA2**, probe sensitivity of **PTQA3** can be affected since the fluorescence signal is weak at the beginning of adding Hg^{2+} ions. In addition, due to the similar fluorescence intensities of **PTQA2** and **PTQA3**, choosing **PTQA2** for sensor performance testing can enhance the sensitivity of fluorescent probe. Then, we studied the sensing properties of **PTQA2** and its nanoparticle (**PTQA-NPs**). The colorimetric sensing properties of **PTQA2** to different metal ions were characterized in the solution of chloroform ($CHCl_3$, 10 μg/mL). Upon addition of Hg^{2+}, shown in Figure 6a, the absorbance at 623 nm and 680 nm were decreased and new absorption peak emergent at 505 nm and 545 nm. Additionally, the shoulder peak at 575 nm was assigned to monothiocarbonyl quinacridone which could be observed in small molecules.[22] The absorption changes of these five peaks were showed in Figure 6b. A small parabolic curve described the absorbance changes at 575 nm indicates generation and disappearance of monothiocarbonyl quinacridone moiety. The magnifying figures showed the characteristic absorbance of thiocarbonyl quinacridone varies with the concentration of Hg^{2+} (Figure 6c ~ 6d). As shown in Figures 6c and d, when the concentration of Hg^{2+} increased from 0 to 7.6 μM, the absorbance was fade-out at 623 nm and 680 nm and fade-in at 545 nm and 575 nm. In this course, dithiocarbonyl component of **PTQA2** transferred to monothiocarbonyl and dicarbonyl ones. With the addition of Hg^{2+} from 7.6 to 14 μM, the peak at 505 nm was emergent and enhanced that indicated generation of quinacridone (Figure 6e). Absorbance at 575 nm decreased in this stage means the monothiocarbonyl component was converted into quinacridone. The peak at 545 nm was still enhanced in this stage and we surmises that it is composed of absorptions of monothiocarbonyl quinacridone and quinacridone. For the same reason, the band at 623 nm is composed of both absorptions of dithiocarbonyl and monothiocarbonyl components that made it

decreased slower than the one at 680 nm. Further investigation of these absorption bands indicated that the dithiocarbonyl quinacridone was first converted to monothiocarbonyl quinacridone and then disulfurized to quinacridone (Scheme 2). Additionally, when Hg^{2+} was added to $CHCl_3$ solution of **PTQA2**, a dramatic color change from green to brown to orange was observed, indicating that thiocarbonyl quinacridone-based sensor can be used as colorimetric probe for naked eye recognition.

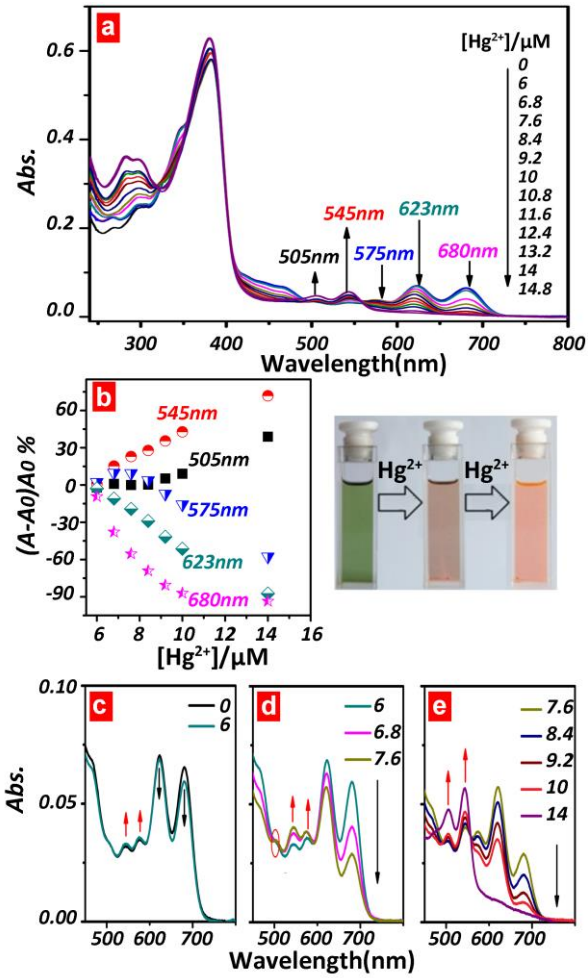

Figure 6. (a~d) UV-vis spectra of **PTQA2** (10 μg/mL) upon the titration of Hg^{2+} in $CHCl_3$; (e) absorbance changes of **PTQA2** with Hg^{2+} at different wavelength.

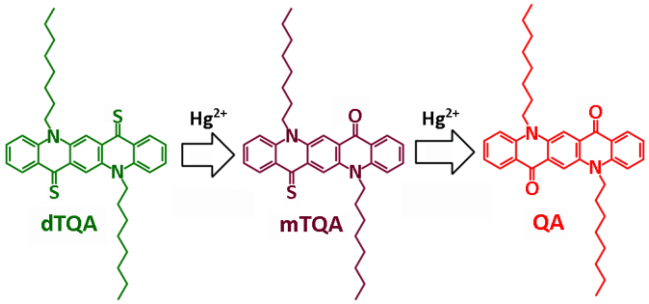

Scheme 2. Sensing mechanism of thiocarbonyl quinacridone-based chemosensors.

Figure 7a showed the fluorescence titration spectra of **PTQA2** with Hg^{2+}. When Hg^{2+} ion was added to the solution of **PTQA2**, about 36-fold emission enhancement at 566 nm was observed. Moreover, the selective studies of **PTQA2** were recorded in Figure 7b and Figure S3a. 14 μM of Hg^{2+} and 40 μM of other metal ions were added to $CHCl_3$ solutions of **PTQA2** and only Hg^{2+} causes about 35 folds emission enhancement at 566 nm.

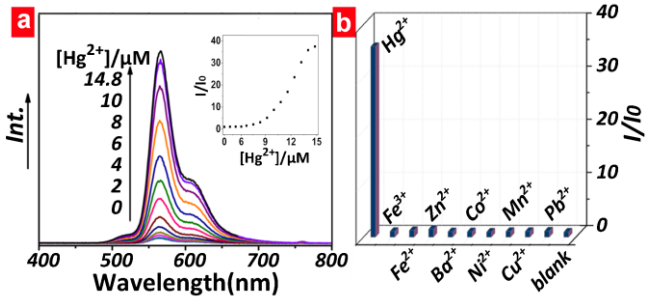

Figure 7. (a) Fluorescent spectra of **PTQA2** (10μg/mL) upon titration of Hg^{2+} in $CHCl_3$ solution.inset: Plot of fluorescence intensity change of **PTQA2** (λ_{ex} = 380 nm, λ_{em} = 566 nm); (b) Selective properties of **PTQA2** towards different metal ions in $CHCl_3$ solution ([Hg^{2+}] = 14 μM and other metal ions [M^{n+}] = 40 μM).

Moreover, the sensing property of **PTQA-NPs** was also studied in the PBS solution (see Figure 8). Differently, a weak emission at 492 nm belonged to fluorene was first observed in the solution of **PTQA-NPs** when nM level of Hg^{2+} was added in the system. Considering of the

aggregation morphology of this nanoparticle, we presumed that the energy transfer process from fluorene unit to thiocarbonyl quinacridone moiety could be disturbed by a little amount of Hg^{2+}. And then, **PTQA-NPs** emitted the fluorescence of fluorene. Upon addition of Hg^{2+}, a new emission at 578 nm was emerged and enhanced for the reproduction of quinacridone groups. The increasing emission at 492 nm indicated that the inefficient energy transfer still occurred in the nanoparticles. Good selectivity was also founded in the PBS solution of **PTQA-NPs** (Figure 8b and S3b). With addition of 14 μM of Hg^{2+}, the emission intensities enhanced 3.56-fold and 32.33-fold at both 492 nm and 578 nm, respectively. To compare with other metal ions, only Hg^{2+} caused distinct fluorescent output. As shown in Figure 8c, the emission intensity of **PTQA-NPs** efficiently increased after 5 μM of Hg^{2+} was added, which means the high sensitivity of the probe.

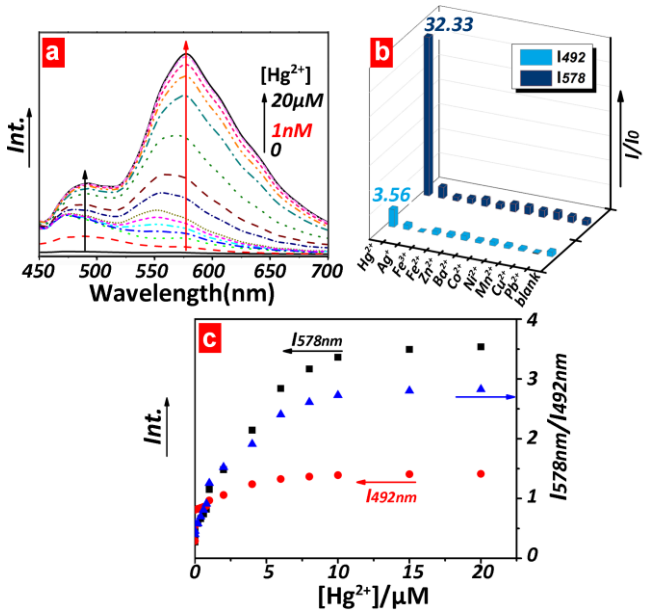

Figure 8. (a) Fluorescent spectra of **PTQA-NPs** (10μg/mL) upon titration of Hg^{2+} in PBS solution; (b) Selective properties of **PTQA-NPs** towards different metal ions in PBS solution ([Hg^{2+}] = 14 μM and other metal ions [M^{n+}] = 40 μM); (c) Plot of fluorescence intensity change of **PTQA-NPs**.

Monitoring Hg^{2+} in Living Cells

After in vitro experiments, we demonstrated the applicability of **PTQA-NPs** in monitoring intracellular Hg^{2+}. The bioimaging experiments were carried out by confocal laser scanning microscopy (CLSM). As shown in Figure 9, HeLa cells incubated with **PTQA-NPs** (10 μg/mL) for 1 h at 37 ^{o}C showed no emission. When the cells were supplemented with **PTQA-NPs** in the growth medium for 1 h at 37 ^{o}C and then incubated with 10 μM Hg^{2+} for 20 min at 37 ^{o}C, a strong enhancement in the red emission was observed in the intracellular region. Bright-field measurements confirmed that the HeLa cells with or without treatment with Hg^{2+} remained viable throughout the imaging experiments. Furthermore, overlay of luminescence and bright field images demonstrated that the red luminescence was evident in the cytoplasm over the nucleus and membrane, which was also confirmed by xz cross-sectional image (Figure S4).

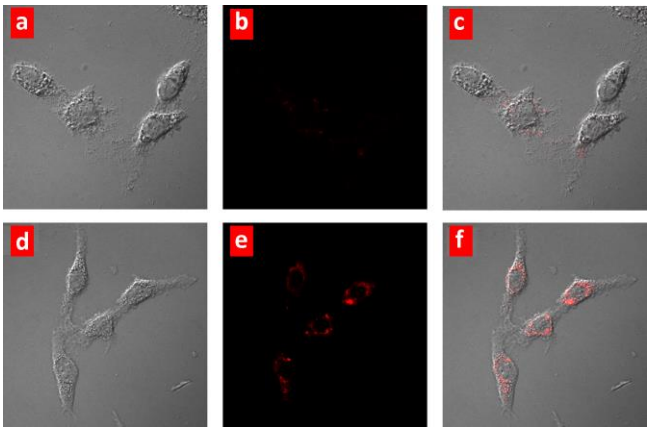

Figure 9. CLSM images in HeLa cells. (Top, a-c) image of HeLa cells incubated with 10 μg/mL **PTQA-NPs** for 60 min at 37 ℃. (a) bright field image; (b) red channel image, and (c) overlay of (a), (b). (Bottom, d-f) image of HeLa cells stained with 10 μg/mL **PTQA-NPs** for 60 min at 37 °C, then further treated with 10 μM Hg^{2+} at 37 ℃ for 20 min. (d) brightfield image; (e) red channel image and (f) overlay of (d), (e). Emission was collected by red channel from 560-660 nm, λ_{ex}= 488 nm.

Conclusion

In summary, we have demonstrated a series of highly sensitive FRET-based thiocarbonyl quinacridone conjugated polymers for sensing and bioimaging of Hg^{2+} ion. The thiocarbonyl quinacridone chromphore, a useful Hg^{2+} sensor, was successfully conjugated with fluorene as an energy donor. For **PTQA2** in chloroform, the addition of mercury ion results in green to brown to orange absorption color change and more than 30-fold fluorescence enhancement at visible region wavelengths. Moreover, this conjugated polymer system could be used for detection of Hg^{2+} in aqueous solution with high sensitivity, which can detect 1 ppb Hg^{2+} in the PBS solution of **PTQA-NPs**. This concentration was lower than the blood level (5.8 ppb) set by the U. S. EPA. Our data confirm that thiocarbonyl quinacridone-based conjugated polymer system is a viable fluorescent probe for Hg^{2+} in biosystem.

Acknowledgements:

This work was supported by NSFC/China (21372082, 2116110444 and 21172073), and the National Basic Research 973 Program (2013CB733700 and 2013CB834701).

References:

1. J. Kaiser, *Science*, 1998, **279**, 1850–1851.
2. D. Zeller and S. Booth, *Science*, 2005, **310**, 777–779.
3. S. E. Bryan, C. Lambert, K. J. Hardy and S. Simons, *Science*, 1974, **186**, 832–833.
4. A. Curley, V. A. Sedlak, E. F. Girling, R. E. Hawk, W. F. Barthel, P. E. Pierce and W. H. Likosky, *Science*, 1971, **172**, 65–67.
5. J. W. Spann, R. G. Heath, J. F. Kreitzer and L. N. Locke, *Science*, 1972, **175**, 328–331.

6. A. H. Stern, *Science*, 2004, **303**, 763–766.

7. V. K. Bains, K. Loomba, A. Loomba and R. Bains, *Br Dent J*, 2008, **205**, 373–378.

8. Q. Xu, S. Lee, Y. Cho, M. H. Kim, J. Bouffard and J. Yoon, *J. Am. Chem. Soc.*, 2013, **135**, 17751–17754.

9. J. Y. Jung, M. Kang, J. Chun, J. Lee, J. Kim, Y. Kim, S.-J Kim, C. Lee and J. Yoon, *Chem. Commun.*, 2013, **49**, 176–178.

10. S. Xu, B. Hu, S. E. Flower, Y.-B. Jiang, J. S. Fossey, W.-P. Deng and T. D. James, *Chem. Commun.*, 2013. **49**, 8314–8316.

11. K. Lawrence, S. E. Flower, G. Kociok-Kohn, C. G. Frost and T. D. James, *Anal. Methods-UK.*, 2012, **4**, 2215–2217.

12. X. Zhou, H. Li, H. Xiao, L. Li, Q. Zhao, T. Yang, J. Zuo and W. Huang, *Dalton Trans.*, 2013, **42**, 5718–5723.

13. H. Son, J. H. Lee, Y.-R Kim, I. S. Lee, S. Han, X. Liu, J. Jaworski and J. H. Jung, *Analyst*, 2012, **137**, 3914–3916.

14. Q. Liu, J. Peng, L. Sun, and F. Li, *ACS Nano*, 2011, **5**, 8040–8048.

15. Y. Yang, Q. Zhao, W. Feng and F. Li, *Chem. Rev.*, 2013, **113**, 192–270.

16. J. Zhang, Y. Zhou, J. Yoon and J. Kim, *Chem. Soc. Rev.*, 2011, **40**, 3416–3429.

17. H. Kim, Z. Guo, W. Zhu, J. Yoon and H. Tian, *Chem. Soc. Rev.*, 2011, **40**, 79–93.

18. X. Chen, T. Pradhan, F. Wang, J. Kim and J. Yoon, *Chem. Rev.*, 2012, **112**, 1910–1956.

19. Y. Liu, M. Chen, T. Cao, Y. Sun, C. Li, Q. Liu, T. Yang, L. Yao, W. Feng and F. Li, *J. Am. Chem. Soc.*, 2013, **135**, 9869–9876.

20. W. H. Ma, Q. Xu, J. J. Du, B. Song, X. J. Peng, Z. Wang, G. D. Li and X. F. Wang, *Spectrochim. Acta, Part A*, 2010, **76**, 248–252.

21. K. C. Song, J. S. Kim, S. M. Park, K. C. Chung, S. Ahn and S. K. Chang, *Org. Lett.*, 2006, **8**, 3413–3416.

22. G. Zhang, D. Zhang, S. Yin, X. Yang, Z. Shuai and D. Zhu, *Chem. Commun*., 2005, **41**, 2161–2163.

23. H. Li, C. Gu, L. Jiang, L. Wei, W. Hu and H. Fu, *J. Mater. Chem. C*, 2013, **1**, 2021–2027.

24. Y. Qu, J. Yang, J. Hua and L. Zou, *Sensor Actuat. B-Chem.*, 2012, **161**, 661–668.

25. C. A. Traina , R. C. Bakus II and G. C. Bazan, *J. Am. Chem. Soc.*, 2011, **133**, 12600–12607.

26. X. Zhou, H. Li, H. Xiao, L. Li, Q. Zhao, T. Yang, J. Zuo and W. Huang, *Dalton Trans.*, 2013, **42**, 5718–5723.

27. J. Song, J. Zhang, F. Lv, Y. Cheng, B. Wang, L. Feng, L. Liu and S. Wang, *Angew. Chem. Int. Ed.*, 2013, **5**2, 13020–13023.

28. J. Liu, Y. Zhong, P. Lu, Y. Hong, J. W. Y. Lam, M. Faisal, Y. Yu, K. S. Wong and B. Z. Tang, *Polym. Chem.*, 2010, **1**, 426–429.

29. R. Hu, J. W. Y. Lam, J. Liu, H. H. Y. Sung, I. D. Williams, Z. Yue, K. S. Wong, M. M. F. Yuen and B. Z. Tang, *Polym. Chem.*, 2012, **3**, 1481–1489.

30. C. Zhu, Q. Yang, L. Liu and S. Wang, *Chem. Commun.*, 2011, **47**, 5524–5526.

31. L. Feng, C. Zhu, H. Yuan, L. Liu, F. Lv and S. Wang, *Chem. Soc. Rev.*, 2013, **42**, 6620–6633.

32. Y. Yuan, R. T. K. Kwok, G. Feng, J. Liang, J. Geng, B. Z. Tang and B. Liu, *Chem. Commun.*, 2014, DOI: 10.1039/C3CC47585A.

33. J. Geng, K. Li, D. Ding, X. Zhang, W. Qin, J. Liu, B. Z. Tang and B. Liu, *Small*, 2012, **8**, 3655–3663.

34. E. Zhao, H. Li, J. Ling, H. Wu, J. Wang, S. Zhang, J. W. Y. Lam, J. Z. Sun, A. Qin and B. Z. Tang, *Polym. Chem.*, 2013, DOI: 10.1039/C3PY01387A.

35. G. Wang, H. Yin, J. C. Y. Ng, L. Cai, J. Li, B. Z. Tang and B. Liu, *Polym. Chem.*, 2013, **4**, 5297–5304.

36. Z. Yang, Y. Yuan, R. Jiang, N. Fu, X. Lu, C. Tian, W. Hu, Q. Fan and W. Huang, *Polym. Chem.*, 2014, DOI: 10.1039/C3PY01197F.

37. A. Levai and J. Jekő, *J. Heterocyclic Chem.*, 2005, **42**, 739–742.

38. J. Liu, B. Gao, Y. Cheng, Z. Xie, Y. Geng, L. Wang, X. Jing and F. Wang, *Macromolecules*, 2008, **41**, 1162–1167.

39. S. W. Thomas, G. D. Joly and T. M. Swager, *Chem. Rev.*, 2007, **107**, 1339–1386.

40. S. Rochat and T. M. Swager, *ACS Appl. Mater. Interfaces*, 2013, **5**, 4488–4502.

For Table of Contents use only

Fluorescent conjugated polymer based on thiocarbonyl quinacridone for sensing mercury ion and bioimaging

Yi Qu,[a,b] Xinran Zhang,[a] Yongquan Wu,[b] Fuyou Li[b] and Jianli Hua[a]**

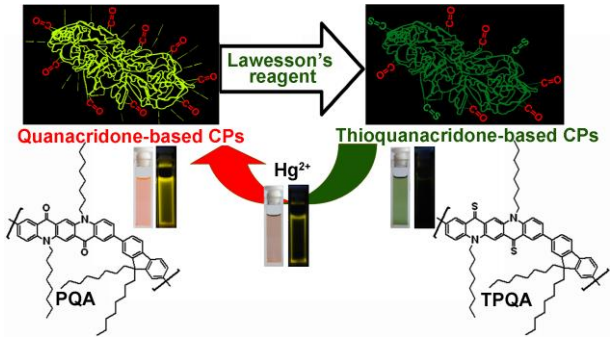

Highly sensitive FRET-based thiocarbonyl quinacridone fluorescent conjugated polymers for sensing and bioimaging of mercury ion have been developed.